



## Improved prediction of bilayer and monolayer properties using a refined BMW-MARTINI force field



Virginia Miguel<sup>a</sup>, Maria A. Perillo<sup>a,\*</sup>, Marcos A. Villarreal<sup>b,\*</sup>

<sup>a</sup> Instituto de Investigaciones Biológicas y Tecnológicas (IIBYT), CONICET - Cátedra de Química Biológica, Departamento de Química-ICTA, Facultad de Ciencias Exactas Físicas, Universidad Nacional de Córdoba, Argentina

<sup>b</sup> Instituto de Investigaciones en Físico-Química de Córdoba (INFIQC), CONICET, Departamento de Matemática y Física, Facultad de Ciencias Químicas, Universidad Nacional de Córdoba, Ciudad Universitaria X5000HUA, Argentina

### ARTICLE INFO

#### Article history:

Received 15 March 2016

Received in revised form 11 August 2016

Accepted 30 August 2016

Available online 31 August 2016

#### Keywords:

Molecular dynamics simulations

Coarse-grained models

Lipid

Bilayer

Monolayer

BMW-Martini

### ABSTRACT

Coarse-grained (CG) models allow enlarging the size and time scales that are reachable by atomistic molecular dynamics simulations. A CG force field (FF) for lipids and amino acids that possesses a polarizable water model has been developed following the MARTINI parametrization strategy, the BMW-MARTINI [1]. We tested the BMW-MARTINI FF capability to describe some structural and thermodynamical properties of lipid monolayers and bilayers. We found that, since the surface tension values of oil/water interfaces calculated with the model are not correct, compression isotherms of lipid monolayers present artifacts. Also, this FF predicts DPPC and DAPC bilayers to remain in the  $L_{\alpha}$  phase at temperatures as low as 283 K, contrary to the expected from their experimental  $T_m$  values. Finally, simulations at constant temperature of bilayers of saturated lipids belonging to PC homologous, showed an increase in the mean molecular area (Mma) upon increasing the chain length, inversely to the experimental observation.

We refined BMW-MARTINI FF by modifying as few parameters as possible in order to bring simulated and experimental measurements closer. We have also modified structural parameters of the lipid geometry that do not have direct influence in global properties of the bilayer membranes or monolayers, but serve to approach the obtained CG geometry to atomistic reference values. The refined FF is able to better reproduce phase transition temperatures and Mma for saturated PC bilayers than BMW-MARTINI and MARTINI FF. Finally, the simulated surface pressure-Mma isotherms of PC monolayers resemble the experimental ones and eliminate serious artifacts of previous models.

© 2016 Elsevier B.V. All rights reserved.

### 1. Introduction

Coarse-grained (CG) models offer the possibility to analyze processes that occur at long length and time scales bypassing the currently available computer power limit, and allow the analysis of system evolution up to the microscale [2,3].

The most commonly used CG force fields (FF) for lipid systems are probably the MARTINI [4] and the Shinoda FF [5]. The MARTINI model was initially developed for lipid systems and further extended to a great variety of macromolecules [2]. This FF is based on a four-to-one mapping, where an average of four heavy atoms plus associated hydrogens is represented by a single bead or interaction center [2]. CG water models group several molecules (usually 3 or 4) into a single unit [1,3,6]. The classic MARTINI CG water model is blind to electrostatic fields and polarization effects since it does not bear charges and interactions between sites are of the Lennard-Jones form [2]. This results in

limitations regarding the screening of electrostatic interactions caused by water. Processes involving movement of charges from a high dielectric environment (e.g. water) to a low dielectric medium (e.g. membrane interior) require a model capable of performing electrostatic screening [6]. Two water models compatible with the MARTINI FF which provide a better representation of the electrostatic interaction have been developed by Yesylevskyy et al. [6] and Wu et al. [1]. These are the MARTINI polarizable water model [6] and the Big Multi-pole Water (BMW) model [1]. Each BMW water groups 4 water molecules into one unit, contains three charged sites, and bears an additional non-electrostatic soft interaction between central sites in different units, using a modified Born-Mayer-Huggins (BMH) potential [1]. Also, a CG BMW-MARTINI FF for lipids and amino acids has been developed by Wu et al. following the MARTINI parametrization strategy and convention [7].

Lipid monolayers are surfactant films formed at hydrophobic-hydrophilic interfaces. The monolayer reduces the surface tension at the interface by shielding unfavorable polar-apolar contacts [8]. Investigation of phospholipid monolayers has biological relevance in the characterization of important biological processes like the regulation

\* Corresponding authors.

E-mail addresses: [mariekator@yahoo.com](mailto:mariekator@yahoo.com) (M.A. Perillo), [mwillarreal@unc.edu.ar](mailto:mwillarreal@unc.edu.ar) (M.A. Villarreal).

of the surface tension of the air–alveolar interface [9] and of Tear Film Lipid Layer (TFLL) [10]. A basic characteristic of surfactant monolayers is their surface tension–molecular area dependence [11]. The isotherm assesses the surface activity and phase behavior of the monolayer [9]. Since surfactant molecules reduce the imbalance of forces at the interface, the reduction in surface tension is larger when the molecular density of the monolayer is higher (the interfacial area is reduced). Therefore, surface tension shows monotonic decrease with increasing surfactant density. An adequate reproduction of surface tension values of lipid monolayers is important for a molecular model, since the surface tension is defined by the balance of forces between the different components of the system. The surface tension depends on the water representation in the given FF [11]. Some CG FFs encounter difficulties when treating gas/liquid interfaces as interfacial surface tension or electrostatic potential are not accurately reproduced and therefore some problems arise in monolayer simulations. It is important to note that the underestimated air–water surface tension offsets the isotherm, and several simulations employed the experimental  $\gamma$  to calculate the isotherm, or introduced an effective surface tension to compensate for the offset [9]. Despite an overall improved performance obtained with polarizable CG water models, quantitative reproduction of the surface tension–molecular area isotherms of lipids monolayers remains difficult [2,8]. MARTINI with polarizable water yields a water/alkane surface tension higher than the calculated value of the water/air interface [6]. Therefore, a water/oil interface behaves as if it actually was made up of two interfaces (water/vacuum and oil/vacuum) close to each other rather than as a single interface [2].

As stated by the developers, BMW-MARTINI FF does not accurately reproduce some mechanical properties of the lipid membranes [7]. When we assessed this FF in order to determine which properties can be accurately described with this CG model, we found that at large mean molecular area (Mma), surface tension of lipid coated water/air interfaces were higher than the surface tension calculated for the free water/air interface, which leads to negative surface pressure ( $\pi$ ) values. Moreover, in simulations of lipid bilayers, we observed that the Mma of saturated phosphatidylcholines (PC) of increasing chain length followed the opposite trend to that observed experimentally. Also, molecular geometries of lipid molecules deviated from the expected based on all atom (AA) FF results. Finally, PC's gel to liquid-crystalline transition temperatures were much lower than expected since all PC lipids were in liquid crystalline state at 283 K.

The main objective of this work is to obtain a CG model that possesses proper treatment of electrostatics while it is capable of better reproducing the thermodynamical and structural properties of the phospholipids systems. We present a version of the BMW-MARTINI FF for lipids in which we improve the performance in the simulation of bilayers and monolayer systems by (i) modifying some beads interactions with water and (ii) by adjusting lipids geometries in order to approach AA models values. It should be mentioned that although further characterization of the re-parametrized FF is necessary for simulations of lipids interactions with peptides, the model improves the reproduction of bilayers and monolayer properties.

A description of the FF re-parametrization is presented in the next section. In the **results and discussion** section we analyze a series of structural and dynamical properties for several phosphatidylcholine (PC) lipids systems, bilayers and monolayer, for the new parameters as well as for the original MARTINI and BMW-MARTINI FFs.

## 2. Simulation methods and models

### 2.1. Parametrization strategy for obtaining a consistent CG model

As mentioned in the **introduction**, while performing simulations with the BMW-MARTINI FF we detected inconsistent results with regard to the surface tension of lipid monolayers and molecular geometry of the lipids. With this in mind, the approach used for the modification

of the FF was to change beads interactions with water as well as the lipids geometries where needed. The changes in beads hydration directly address the surface tension of the system. On the other hand, modified lipid geometries, besides a direct structural effect, can reshape interactions in an indirect fashion, for example making more (or less) accessible a given moiety to the surrounding environment. To re-parametrize the interactions with water, we compared our results to experimental data such as surface pressure–mean molecular area ( $\pi$ -Mma) values of monolayer isotherms, Mma in bilayers and gel to liquid transition temperature ( $T_m$ ). For the molecular geometries we adjusted bonds and angles based on results obtained with AA and united-atom (UA) simulations. For the molecular geometries the general approach of MARTINI developers was used, i.e., AA or UA simulations were first converted into a “mapped” CG simulation by identifying the center-of-mass of the corresponding atoms as the CG bead [12]. In this case the AA Stockholm Lipids (Slipids) [13] and the UA Gromos 43A1-S3 [14–16] were used as a reference since they are known to reproduce structural data obtained experimentally through X-ray and neutron diffraction.

MARTINI CG phosphatidylcholine (PC) lipids consist of hydrophobic tails of C1 type beads, Na beads of intermediate polarity to represent glycerol moiety, a negatively charged Qa bead for the phosphate group, and a positively charged Q0 bead for the choline group [12]. Double bonds in the tail are modeled using fewer hydrophobic beads (C2, C3) along with a change of the angle bending potential of the lipid tails [12]. C1 beads are the same constituent particles of the alkanes. As mentioned in the **introduction**, surface tension at the water/alkane interface is incorrect for CG MARTINI and BMW models. Therefore, our first step was to improve the surface tension of long hydrocarbon chains. This was achieved by increasing C1 beads hydration. Also, the effect of increasing phospholipids glycerol beads (Na) hydration was assessed. We did not introduce any additional modifications among other bead interactions (i.e. C1-Na or Na-Na, etc.). Although further modifications that could improve MD reproduction of experimental data are not discarded, we were able to significantly improve the performance of the FF by simply modifying hydration values.

After each round of parametrization scheme, it was necessary to refit the structural potentials until self-consistency was obtained. As in any simplified model there is always a trade-off in reproducing different properties of the system. In this work, we have given priority to more global properties such as Mma for PC lipids series over molecular geometries.

### 2.2. Molecular dynamics simulation details

MD simulations of bilayers of pure DLPC phosphatidylcholine lipids were performed using the Slipids [13] and Gromos 43A1-S3 FFs [14]. A fully solvated, and equilibrated with the corresponding FF, bilayer containing 128 and 100 lipid molecules were used for Slipids and Gromos respectively. The simulation protocols were the same as in the original references. For simulations with Slipids we used the parameters available in the Stockholm lipids home page (<http://mmkluster.fos.su.se/slipids/Downloads.html/>). For the simulations with the Gromos FF the parameters and equilibrated initial structures were obtained from Lipidbook [17] (<http://lipidbook.bioch.ox.ac.uk>). Simulations of 100 ns in the NP<sub>xy</sub>P<sub>z</sub>T ensemble ( $N$  = the number of molecules,  $P_{xy}$  and  $P_z$  are the transverse and normal components of the pressure tensor respectively) were collected for all the systems; the final 70 ns of these simulations were employed for analysis.

For CG models, the effect of increasing hydrocarbon chains length in the Mma of saturated PC lipids was measured using bilayers of DLPC (1,2-didodecanoyl-*sn*-glycero-3-phosphocholine 12:0/12:0), DPPC (1,2-dihexadecanoyl-*sn*-glycero-3-phosphocholine; 16:0/16:0) and DAPC (1,2-Diarachidoyl-*sn*-glycero-3-phosphocholine; 20:0/20:0). We also analyzed bilayers of the monounsaturated lipid DOPC

(1,2-dioleoyl-sn-glycero-3-phosphocholine; 18:1/18:1). The Mma of lipid bilayers was calculated from simulations in the  $NP_{xy}P_zT$  ensemble. Patches of 512 lipids were simulated with a hydration level of 15 CG waters per lipid. Mma was obtained as  $Mma = A_{xy}/N$ , with  $A_{xy}$  being the total area at the xy plane and N the number of lipids in each monolayer. For the determination of the main transition temperature ( $T_m$ ), we performed a series of 200 ns simulations of lipid bilayers in the  $NP_{xy}P_zT$  ensemble at different temperatures with a  $\Delta T = 10$  K, and followed the Mma as a function of time for each temperature.  $T_m$  was set as the temperature where Mma changes drastically in the simulation. This change is due to the marked difference in Mma of lipids in the gel and disordered fluid phases and is easily noticed. The  $T_m$  determination has an associated error of  $\pm 10$  K.

$\pi$ -Mma compression isotherms were obtained for pure lipid monolayers using MARTINI [4], BMW-MARTINI [7], or our own modifications of the BMW-MARTINI FF. Compression isotherms of pure DLPC, DPPC, DAPC and DOPC monolayers were simulated. The system setup consisted of two independent monolayers of 128 lipids each, separated by a water slab of 80 Å. In order to avoid interactions between the monolayers, the system cell was elongated to 300 Å. In Fig. S1 a representative equilibrated structure for the monolayers is presented. A set of initial structures with different areas per lipid in the monolayer was prepared using the PACKMOL software [18]. In this way the asymmetrical distribution is avoided. Depending on the Mma simulated, the number of water beads was between 5000 and 10,000, with more molecules needed for the larger areas. The compression isotherm was calculated by simulating the systems at every Mma for 100 ns in the NVT ensemble and calculating the average surface tension (see below). Constant-area simulations as in the NVT ensemble give reasonable results if the starting conditions are well equilibrated [19]. The temperature was maintained constant using the V-rescale thermostat [20] with a coupling constant of 0.4 ps. Water and lipids were included in separate temperature coupling groups. The Parrinello-Rahman algorithm was used for semi-isotropic pressure coupling with a time constant of 12.0 ps. Non-bonded interactions were treated as described in the original publications [1,4]. Basically the Lennard-Jones interactions were shifted, while the Coulombic interactions are also shifted in the MARTINI FF, but are calculated with the PME method [21] in the BMW-MARTINI FF. A time step of 20 fs was used and the neighbor list was updated every 10 steps. The simulations were 100–200 ns long.

The surface tension in the system was calculated as before [22], from the difference between the normal,  $P_N$ , and lateral,  $P_L$ , pressures in the box.

$$\gamma = (P_N - P_L)L_z/2$$

Here  $L_z$  is size of the box in the direction normal to the interface and  $P_L = (P_{xx} + P_{yy})/2$ .

The corresponding surface pressure is given by the relation:  $\pi(Mma) = \gamma_{wa} - \gamma_m(Mma)$ , where  $\gamma_{wa}$  denotes the surface tension of the water/air interface and  $\gamma_m(Mma)$  is the surface tension of the monolayer coated water/air interface at a given Mma [19].

The surface tension value of BMW and MARTINI polarizable water models are 77.4 mN/m and 30.5 mN/m, respectively. These values were confirmed with a 50 ns simulation of pure water and are in agreement with the ones originally published by the developers [1,6].

Note that the simulation times indicated for the MD simulations are the actual values. The effective time is expected to be near 4 times longer, since CG models result in a speeding up of the kinetics of the system [2]. The effective times are the physically meaningful.

Monolayer collapse was defined as monolayers with a surface tension higher than the surface tension of water/air of the respective model. Phospholipid phases were assigned following general procedures described in the literature; LE is the liquid expanded phase, LC is the liquid condensed phase and LE-LC is the coexistence of LE and LC [23].

Free energy profile calculations were derived from the PMF  $\Delta G(z)$  calculation as a function of the distance of the PO4 bead of the translocating lipid to the bilayer center along the z-axis normal to the plane of the bilayer. A series of 20 separate simulations, of 10 ns each, was performed, in which the PO4 bead of the translocating lipid was restrained to a given depth in the bilayer by a harmonic restraint on the z-coordinate. A force constant of 1000 kJ/mol nm<sup>-2</sup> was used with a spacing of 0.1 nm between the centers of the biasing potentials. The Weighted Histogram Analysis Method (WHAM) was used to extract the PMF and calculate  $\Delta\Delta G$  [24].

Simulations were performed using the GROMACS simulation package (version 4.5.5) [25].

### 3. Results and discussion

#### 3.1. Surface tension at the oil-water interface

Lipids chains are modeled in MARTINI as a linear chain of hydrophobic (C) beads, the same constituting beads of the alkanes [4]. Alkanes have proven to be a valid model for the representation of lipids hydrophobic tails [13]. Baron et al. [26] analyzed the behavior of hydrocarbons of increasing chain length using the MARTINI FF and found that oil/oil interactions are too weak, and water/oil repulsion is overestimated for the model. The same is observed for BMW-MARTINI [7]. Hydration free energies for butane are ~10 kJ/mol, in correspondence with the expected values for AA force-fields (~10 kJ/mol), but deviate considerably for larger alkanes, reaching energies values up to ~15 kJ/mol larger than the expected for hexadecane [7]. Similarly to the original MARTINI model [4], BMW-MARTINI model systematically overestimates the hydration free energies as compared to experimental values [7]. The magnitude of the overestimation is larger for more polar beads (i.e., P groups) [7]. Table 1 shows the surface tension values obtained for the original MARTINI, the BMW-MARTINI and with our modified FF along with experimental values for water/air, hexadecane/air and water/hexadecane interfaces. It can be observed that the calculated surface tension at the hexadecane/air interface is comparable to the experimental values. Water/air values are comparable to experiment for the BMW model, but they are too low in the MARTINI FF. None of the simulated models gives a quantitative approximation to the experimental values for the water/hexadecane system. However, it is more important to note that for both MARTINI and BMW-MARTINI models, the water/hexadecane surface tension is even larger than for the water/air system. The fact that in mixed systems, the surface tension is larger than the surface tension of pure systems lacks physical sense and, in this case, indicates poor water-alkane interactions. Only our modified BMW FF gives surface tension values for the water/hexadecane interface that are closer the values obtained for the pure systems (see Table 1). Considering that a lipid monolayer at the water/air interface is expected to reduce the surface-tension between these two phases, and that at large Mma the lipid tails are exposed to water to some degree, it is expected that the reproduction of the  $\pi$ -Mma isotherms may present some challenges [2]. Limitations for the reproduction of pressure-area isotherm for lipid monolayers using MD simulations have been characterized before [22].

**Table 1**

Theoretical and experimental surface tension values of referent interfaces. Values are in mN/m.

	Hx	W	W/Hx
Experimental	27b	72b	55c
MARTINI	24	31	40
BMW-MARTINI	24	79	93
This work	23	79	69

Hx = hexadecane/air. W = water/air. Hx/W = water/hexadecane.

b) <http://webbook.nist.gov/>.

c) [27].

Simulated  $\pi$ -Mma compression isotherms of monolayers of PC lipids were performed using the original BMW-MARTINI FF [7] in order to determine if it is able to reproduce experimental  $\pi$ -Mma isotherms. The resulting isotherms of DOPC are shown in Fig. 1.  $\pi$  values obtained from CG simulation show some physical inconsistencies, such as the fact that at high Mmas (near 90 Å<sup>2</sup>/lipid)  $\pi$  values were negative, which makes no physical sense. As the Mma is increased and the lipids adopt less ordered configurations, hydrocarbon chains become more exposed to water, making the interface more similar to the water/oil interface. This is the cause of the observed behavior at high area/per lipids values, where surface tension of BMW-MARTINI lipids coated interfaces is higher than the surface tension calculated for the free water/air interface, which leads to negative  $\pi$  values.

We attempted to recalibrate long chain alkanes in order to reproduce lipid hydrophobic tails. The strength of the interaction, determined by the value of the well-depth  $\epsilon_{ij}$ , depends on the interacting particle types. Original MARTINI values for the well-depths,  $\epsilon$ , between uncharged bead types and water were modified in BMW [7] using scaling factors. We will refer to these values as scaled interactions. In order to achieve proper hydration, epsilon value for water-alkane interaction (P7-C1 interaction) was modified from a “scaled-repulsive” (1.42 kJ/mol) to a “semi-repulsive” (2.7 kJ/mol) interaction value (Table 2). This positions water/alkane surface tension values between water/air and alkane/air surface tension values, as required.  $\pi$ -Mma isotherms were calculated for DOPC, using the modified C1 hydration values (Fig. 1, green line). Further increase of water-alkanes interactions could improve these values, but would disturb hydrophilic-hydrophobic balance in the FF and would require an intensive re-parametrization and the possible addition of new interactions.

After several rounds of parametrization, an increase in the hydration of the glycerol beads was necessarily favored in order to eliminate negative values in the  $\pi$ -Mma curves. Glycerol beads hydration was favored by increasing water-glycerol beads epsilon values from “scaled semi-repulsive” (2.84 kJ/mol) to “almost-attractive”

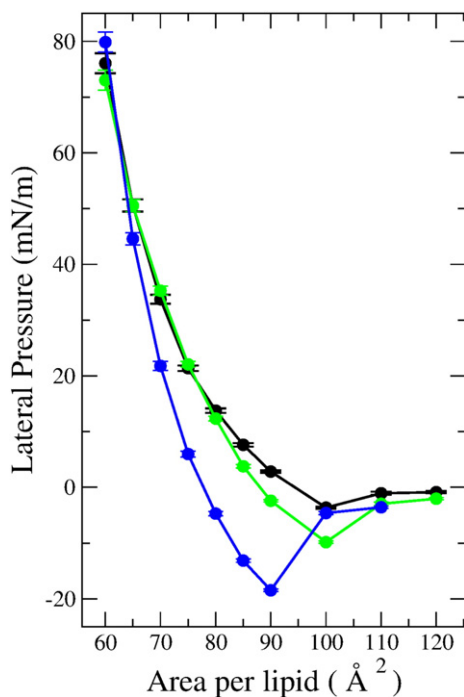


Fig. 1.  $\pi$ -Mma isotherms for DOPC calculated using the original BMW-MARTINI force field (blue line), modifying hydrophobic tail-water interaction, (green line) and modifying hydrophobic tail- and also glycerol-water interaction (black lines). For both of the curves with modified hydration values, lipids geometries were also changed to the final values detailed in Table 2 (see below).

Table 2

Beads hydration values. Interaction of P7 water bead type with lipid beads.

	BMW-MARTINI	This work
C1	1.42	2.7
Na	2.84	4.5

Values in kJ/mol.

(4.5 kJ/mol) (Table 2).  $\pi$ -Mma isotherms were calculated for DOPC, using the modified C1 and Na hydration values (Fig. 1, black line).

### 3.2. Phosphatidylcholine lipids structural properties

Structural comparison of CG models with AA and experimental data is useful for the optimization of the bonded interactions of the former. We evaluated the BMW lipid models by comparison to CG MARTINI and AA simulations using the Stockholm (Slipids) [13] and GROMOS 43A1-S3 lipids [14]. Simulation of DLPC and DOPC bilayers at 323 K, was used in this comparison. We mapped AA lipids chemical structure to the CG representation following the MARTINI Coarse Graining approach, and these structural parameters were used as parametrization targets. The mapping of CG particle types is showed in Fig. 2. In CG FFs, beads mapping limits the chemical resolution and the accuracy of structural details [2]. In some cases the modifications of the local structure of the lipids have pronounced influence on the global structure of the lipid bilayer properties such as Mma, surface tension, melting point, and therefore a compromise has to be achieved between the fine-tuning of lipid geometries and the reproduction of global properties. In such cases we have preferred a closer reproduction of global vs local properties.

The values of the molecular geometry obtained with the original BMW-MARTINI showed several discrepancies with respect to AA data. Particularly, the bond distance between phosphate and choline head groups (P-N) was quite longer than expected according AA models, and also when compared to original MARTINI (Fig. 3). The P-N distance distribution obtained with Slipids presents narrow distribution with a single maximum centered at 4.4 Å, while for the GROMOS 43A1-S3, the distribution is bimodal with maximums at 4.5 and 4.9 Å. While MARTINI has a distribution compatible with the AA results, for BMW-MARTINI the observed mean value was 6.8 Å which is too long (Fig. 3).

BMW-MARTINI FF developers used the structural parameters taken straight from the original MARTINI without any further re-

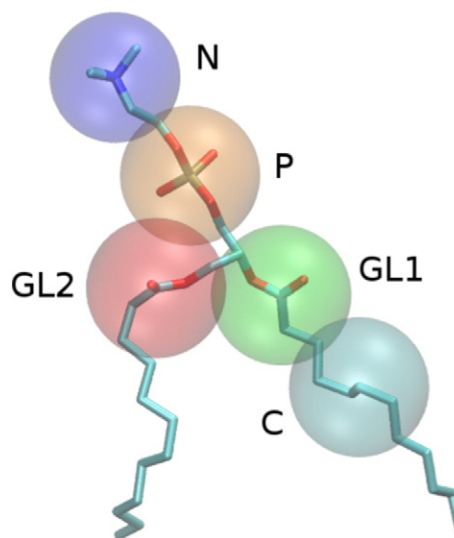
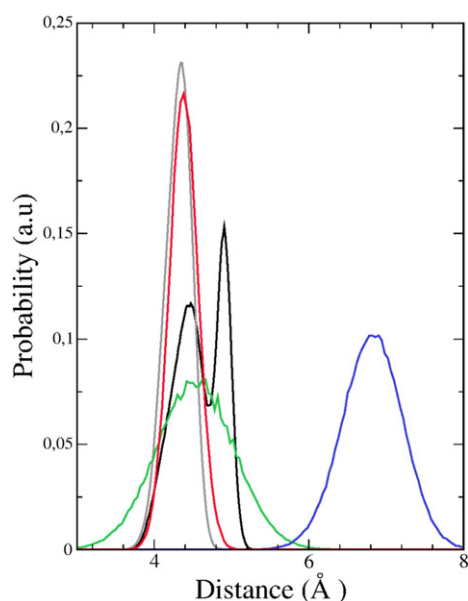


Fig. 2. All Atom to coarse grained mapping of the chemical structure of PC lipids. The all atom structure is shown in sticks while the coarse grained beads are shown as transparent vdW spheres.



**Fig. 3.** Phosphate-choline (PO<sub>4</sub>-NH<sub>3</sub>) bond length distribution calculated for Stockholm lipids (gray line) and GROMOS (black line) FFs as well as GC MARTINI (green line), BMW-MARTINI (blue line) and our modified FF (red line).

parametrization [7]. Not all structural parameters of MARTINI FF are expected to work properly if the water model is modified, especially for molecular moieties with strong interaction with water. It is clear from Fig. 3 that this is the case of the P-N bond in the lipid head group, which, due to the strong interaction with the BMW water, adopts a larger equilibrium distance. The mean distance between P and N of 6.8 Å in the BMW model is long enough for a water bead to insert in between. Clearly a re-parametrization is needed for this bond. PC lipids are neutral, but carry an electric dipole moment since the PO<sub>4</sub> and NH<sub>3</sub> groups are charged, bearing negative and positive charge, respectively. This makes P-N bond distance play a key role in the regulation of global behavior of CG lipids. For instance, we noticed that a reduction in this bond length reduces lipids *Mma*. We explain this through its influence on the regulation of interaction of the polar head beads with water. At short bond length, lipid-lipid interactions predominate over polar head-water interactions and the bilayers contracts. The opposite situation favors polar head-water interactions and the membrane tends to expand. Different hydration levels of the polar head groups determine different values of the surface potential and the dipole potential [28]. Therefore, P-N beads distance bond is involved in the determination of the interface potential that ultimately regulates long distance domain interactions. We modified the P-N bond length in the BMW-MARTINI by increasing the spring constant and reducing the equilibrium distance. The obtained distribution is in good agreement with the one obtained with the Slipids (Fig. 3).

An additional molecular parameter with clear incidence on global properties of the bilayer is the geometry of the carbon beads of the hydrophobic tails of the lipids, especially angle bending, which is crucial in order to obtain an accurate melting temperature and *Mma* of the bilayer. We found that making the lipid chain straighter increases the attraction between lipid chains, which diminishes the *Mma* and increases the melting constant of the lipid bilayer. It is possible to make the chain straighter by increasing the spring constant of the bending of the angle C-C-C. In our final parameter we have increased the bending constant by a factor of almost three. This modification is further discussed in Section 3.3. Also, it is important to take into account the P-GL1-C1 angle. We have observed that when the equilibrium value of this angle is reduced an increase of the *Mma* is produced, although we have no clear explanation for this behavior.

We have also modified other structural parameters of the lipid geometry that do not have direct influence on global properties of the membranes or monolayers, but serves to approach the obtained CG geometry to the AA reference values. The criterion used was not to exactly match the AA distribution but to keep the number of the parameter changes to a minimum. In Fig. S2 we show the comparison of the distributions for different bonds and bending. Table 3 and Table 4 show the topological parameters modified in this work, along with the original values for comparison. The BMW-MARTINI share the same geometrical parameters except where indicated. Modified FF parameters are available as supplementary material (see *BMW Modified topologies*).

### 3.3. Phase transition temperature (*T<sub>m</sub>*) for lipid bilayers from gel to liquid-crystalline

We analyzed the phase transition temperature of typical saturated PC bilayers (DPPC and DAPC) [29] to determine whether BMW-MARTINI FF is suitable to capture the main phase transition temperature. We performed a series of simulations of each lipid bilayer system starting from previously equilibrated structures in the gel phase (*L<sub>β</sub>*) and then proceeded with the melting of the ordered *L<sub>β</sub>* phase towards a disordered fluid phase (*L<sub>α</sub>*). The *L<sub>β</sub>* differs from the *L<sub>α</sub>* phase by a lower *Mma* and a strongly reduced lateral mobility, among other key features [30,31]. We followed the *Mma*, that is sensitive to the phase state of the bilayer, to determine the melting temperature [32]. Due to the approach followed to determine the melting temperature its determination is not precise for our MD simulations. Therefore, a *T<sub>m</sub>* range is given (see Table 5).

The estimated transition temperature of DPPC in the BMW-MARTINI is 283 K, and in the 313 to 323 K degrees range for MARTINI and our model. It should be noticed that 283 K is the lowest temperature we were able to test for BMW FF since at lower temperatures water is expected to freeze. Therefore, in practice BMW bilayers of DPPC are always at the *L<sub>α</sub>* phase. Experimentally, DPPC has a pre-transition temperature (*T<sub>pre</sub>*) of 307 K, which is not captured by any of the FF tested, and a main phase transition temperature (*T<sub>m</sub>*) of 314 K [30,31,33]. In the case of DAPC the BMW-MARTINI bilayers are also always in the *L<sub>α</sub>* phase, while the MARTINI and our model are closer to the experimental value [29]. In this case the MARTINI model gives a *T<sub>m</sub>* lower than the experimental while for our model the *T<sub>m</sub>* is higher (see Table 5). The temperature difference between the gel-to-fluid transitions in the BMW-MARTINI CG model versus experimental DPPC is 30 K and almost 50 K for DAPC, while with our re-parametrization the difference is on the order of 10 K.

The bonded parameters for BMW-MARTINI model are the same as the original MARTINI, with the only modification of the force constant for angle bending in lipid tails, which is reduced from 25 to 10 (kJ/mol deg<sup>-2</sup>) [7]. BMW-MARTINI developers justify this modification because of the narrower angle distribution in MARTINI when compared to AA models [7,26]. The reduced force constant in BMW-MARTINI increases hydrocarbon chain flexibility that ultimately affects melting temperatures. As mentioned before, during parametrization we observed that an increased angle bending force constant for lipid tails (C-C-C angle) correlated with an increase in the melting

**Table 3**

Comparison between the original and new parameters for the bond stretching.

	BMW-MARTINI		This work	
	<i>r</i> <sub>0</sub>	<i>k</i> <sub>0</sub>	<i>r</i> <sub>0</sub>	<i>k</i> <sub>0</sub>
N-P	4.7	1250	4.0	8000
P-GL1	4.7	1250	4.0	2000
GL1-GL2	3.7	1250	4.0	2000
GL1-C	4.7	1250	4.8	2000
C-C	4.7	1250	4.8	2000

*r*<sub>0</sub> - equilibrium distance (Å). *k*<sub>0</sub> force constant (kJ mol<sup>-1</sup> Å<sup>-2</sup>).

**Table 4**

Comparison between the original BMW-MARTINI and new parameters for the angle bending.

	BMW-MARTINI		This work	
	$a_0$	$k_0$	$a_0$	$k_0$
N-P-GL1	–	–	100.0	7.0
P-GL1-GL2	120.0	25.0	100.0	50.0
P-GL1-C	180.0	25.0	130.0	50.0
GL1-C-C	180.0	10.0 (25.0)*	180.0	80.0
C-C-C	180.0	10.0 (25.0)*	180.0	80.0
C = C-C	120.0	45.0	130.0	60.0

$a_0$  – equilibrium angle (Deg).  $k_0$  force constant ( $\text{kJ mol}^{-1} \text{Deg}^{-2}$ ). \* Values in parenthesis are for the MARTINI FF.

temperature. Using a stiffer bond-angle potential the chain tends to be more elongated therefore favoring a stronger inter-chain interaction, which translates in a higher  $T_m$ . By increasing force constant we were able to obtain  $T_m$  values for DPPC and DAPC, although still high, closer to the experimental ones than with the original MARTINI FF (see Table 5).

### 3.4. Mean molecular area of bilayers in the homologous PCs series

MD simulations of lipid bilayers require a precise description of the Mma and this is often used as the key parameter when assessing the validity of MD simulations of lipids. We evaluated the molecular area of saturated lipids with increasing hydrocarbon chains length for the PC homologous series (Fig. 4). Hydrocarbon chains mapping of DLPC, DPPC and DAPC lipids in BMW-MARTINI consist of 3, 4 and 5 beads respectively. It should be taken into account that for these CG models, DLPC and DMPC for one side, and DSPC and DAPC, for the other, cannot be distinguished due to the resolution employed in the mapping (Fig. 2.)

All lipid systems were simulated at different temperatures. At a given temperature a decrease in lipid area as a function of increased chain length is expected. This behavior is the consequence of larger van der Waals attractive forces between the hydrocarbon tails with longer lipid chain length [34]. For example, lipid areas of DLPC, DPPC and DSPC bilayers determined using small-angle neutron and X-ray scattering data at 333 K are 65.9, 65.0 and 63.8  $\text{\AA}^2$ , respectively [34]. Inversely to the experimental observation, lipid areas of simulated bilayers with both MARTINI and BMW-MARTINI FF presented an increase in Mma as chain length increases (see Fig. 4).

During parametrization we observed that the bending constant for C-C-C angle influenced not only the  $T_m$ , but also the Mma. With the modifications introduced by us to the BMW-MARTINI FF, we obtained values for Mma that qualitatively reproduced the expected behavior of PC lipids of increasing length (Fig. 4). Experimentally, DLPC and DPPC lipids differed by a Mma of 1 to 1.7  $\text{\AA}^2$  depending the temperature of comparison (E.E. Ambroggio and M.L. Fanani, personal communication). With our modified FF, this difference is near 2.5  $\text{\AA}^2$ , which is within the uncertainties of both experimental and simulation results.

The slope of Mma vs temperature curve corresponds to the coefficient of thermal expansion, which describes the tendency of the bilayer to change in volume in response to a change in temperature [36]. This is well described by MARTINI FF, since Mma vs temperature curve slope is

**Table 5**

Theoretical and experimental  $T_m$  values for PCs of different chain lengths.

	BMW-MARTINI ( $k_0^a = 10$ )	MARTINI ( $k_0 = 25$ )	This work ( $k_0 = 80$ )	Experimental
DPPC	283 <sup>b</sup>	313–323	313–323	314[33]
DAPC	283	323–333	343–353	339[29]

<sup>a</sup> Values in  $\text{kJ mol}^{-1} \text{deg}^{-2}$ .

<sup>b</sup> Values in Kelvin.

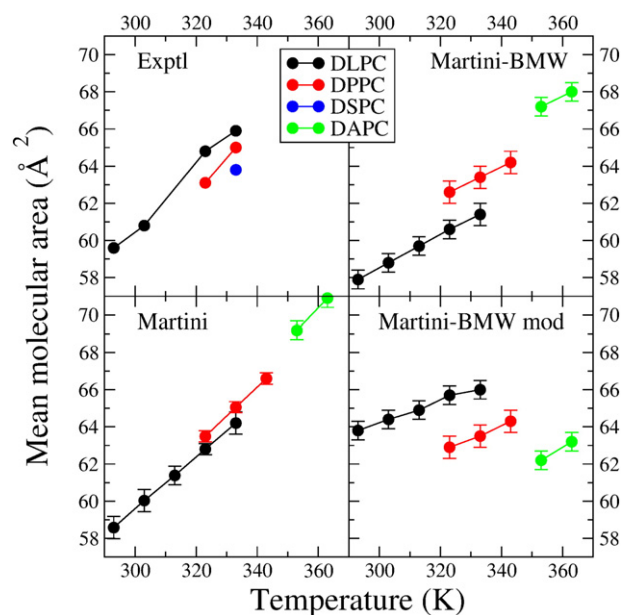


**Fig. 4.** Mma obtained for a homologous series of saturated PC lipids of increasing chain length as a function of temperature. Experimental values were taken from [34,35]. Simulations using CG MARTINI and BMW-MARTINI models were also compared to our modified BMW-MARTINI. All simulated values were calculated in this work.

similar to the experimental one, while BMW-MARTINI and our modified FF are less sensitive to temperature changes (see Fig. 4).

Two additional elastic and dynamic properties were computed in order to test the ability of the modified FF to reproduce experimental data for lipid bilayers. Since an ensemble of different experimental values can verify the FF, Isothermal area compressibility modulus (KA) and Lateral diffusion coefficient (D) were calculated. The lipid lateral diffusion rate can be calculated from an MD trajectory from the slope of the mean squared displacement (MSD). The diffusion coefficients obtained from the slope of the MSD curve were included into supplementary material (table S1) and compared to those calculated for Slipids [13], MARTINI [4] and experimental values. For DPPC in the fluid phase in the MARTINI model, the diffusion coefficients are in the range  $10\text{--}40 \times 10^{-8} \text{ cm}^2 \text{ s}^{-1}$  for the temperature range  $T = 285\text{--}350 \text{ K}$  [30]. Experimental values for DPPC are  $6\text{--}2 \times 10^{-8} \text{ cm}^2 \text{ s}^{-1}$  between  $T = 315\text{--}335 \text{ K}$  [37] and  $10 \times 10^{-8} \text{ cm}^2 \text{ s}^{-1}$  at  $T = 321 \text{ K}$  [38]. We obtained values for DPPC of  $16\text{--}32 \times 10^{-8} \text{ cm}^2 \text{ s}^{-1}$  between  $T = 323$  and  $343 \text{ K}$ . Therefore, the range of diffusion rates obtained for the modified BMW overlap with most of the experimental, MARTINI and Slipids measurements.

### 3.5. MD simulations of $\pi$ -a compression isotherms of pure PC lipids

$\pi$ -Mma isotherms were calculated for saturated PC lipids DLPC, DPPC and DAPC. Simulations of CG are included here, using the MARTINI, BMW-MARTINI and our own new modified FF (see Fig. 5). The main result for this section is that with the modifications made, we were able to remove the region of negative values of surface pressure that are present in the isotherms of both MARTINI and BMW-MARTINI. As mentioned before, these negative regions are unphysical since this situation would indicate that the surface tension of the interface in the presence of the lipids monolayer is higher than that of the pure water. We attributed this behavior to a poor alkane-water interaction, also reflected in a water/alkane surface tension value not lying in between the water/air and alkane/air surface tensions.

The modifications introduced not only allowed for the elimination of this serious artifact, but also another inconsistency in regard to the effect of the chain-length. Due to the longer tail, experimental DPPC isotherms are more condensed than that of DLPC. This is not reproduced by

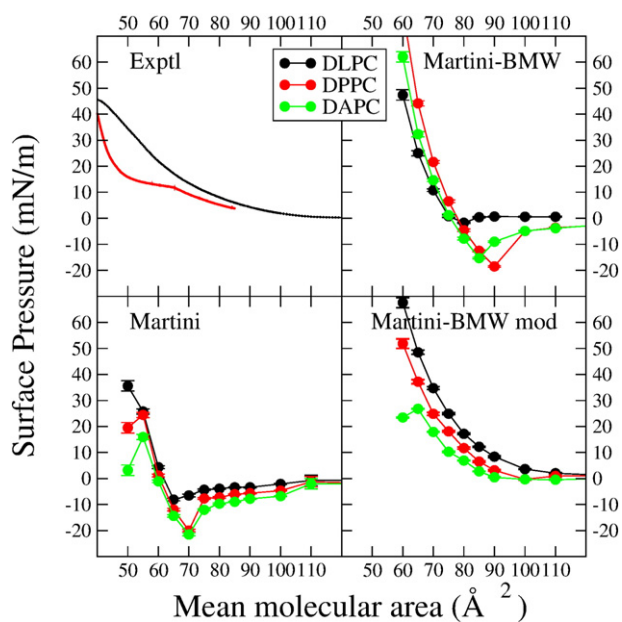


**Fig. 5.** Compression isotherms of DLPC, DPPC and DAPC. Theoretical data were calculated with MARTINI, BMW-MARTINI and our modified FF and compared with experimental data (E.E. Ambroggio and M.L. Fanani, personal communication).

the BMW-MARTINI where DPPC isotherms are slightly more expanded than DLPC, but is well described in both the MARTINI and our modified FF.

Nevertheless, when simulated isotherms are compared with experimental ones in detail, it can be seen that theoretical isotherms are shifted to areas/lipid larger than those obtained experimentally, especially at high surface pressures. The shift of the simulated isotherms to larger Mma with respect to experimental ones occurs for CG and AA simulations alike [19]. Moreover, while experimental DPPC  $\pi$ -Mma isotherm presents prominent liquid expanded (LE) and liquid condensed (LC) states and a LE-LC coexistence region (see Fig. 5), isotherms simulated by all the FFs tested lack LC-LE coexistence.

Isotherm simulated with MARTINI model has previously shown to present LC-LE phases coexistence plateau at 300 K [22]. The discrepancy between our MARTINI results and the previous work by Baoukina et al. is most probably due to system size [22]. The presence of LC/LE coexistence in DPPC isotherms is supposed to depend on temperature and system size [39]. In order to explore the possibility of our modified BMW-Martini FF to show LC-LE coexistence we expanded the range of temperature used for DPPC pressure-area isotherm to 285–313 K and increased our system size to 1100 DPPC molecules/monolayer, and still found no evidence for the LC/LE transition (data not shown). It should be pointed out that the original BMW-MARTINI FF has no reports of being capable to reproduce DPPC LC/LE transition.

Finally, the slopes of the surface pressure-area isotherms of the monolayer, a parameter proportional to the area compressibility modulus,  $K_A$ , are somewhat flatter with our modified FF compared to Martini and BMW-Martini FF curves (Fig. 5). Membrane lateral compressibility is important for proper cell function since it determines the capacity of elastic membrane deformation. Therefore, we calculated the  $K_A$  values obtained with our modified FF and compared it with original and Slipids monolayers (see SFig. 3).  $K_A$  values were calculated from  $\pi$ -A isotherms data. Calculated values for the monolayer  $K_A$  in the LE phase using the MARTINI model agree well with experimental values [22]. The maximum values of DPPC  $K_A$  values vary between models from  $K_A = 350$  (at  $A_L = 0.65$  nm) in BMW-MARTINI;  $K_A = 212$  (at  $A_L = 0.60$  nm) in MARTINI and to  $K_A = 200$  (at  $A_L = 0.65$  nm) in our modified FF (see SFig. 3).

### 3.6. DPPC free energy of lipid desorption and flip flop

We tested the ability of our model to reproduce lipid translocation (flip-flop) free energies and lipid desorption from the bilayer into bulk water. We determined the free energy barrier for lipid flip-flop, and the free energy for lipid desorption using umbrella sampling in liquid-disordered bilayer calculating the potential of mean force (PMF) (Fig. 6A). The free energy for DPPC flip-flop and pore formation for atomistic model presents energy barriers of ca. 80 kJ/mol [40]. According to Bennet and Tileman there is good agreement between the AA and CG MARTINI models on the shape of the PMFs and the free energy barriers for DPPC, but found that the free energy barriers for BMW-MARTINI DPPC flipflop are significantly overestimated [40]. The BMW water model presents a steeper slope in the PMF and a significantly higher barrier for flip-flop, although the position of the free energy minima is the same as the other two CG models [40]. We confirmed this observations, since we obtained an energy barrier of approx. 115 kJ/mol with original BMW FF (Fig. 6A), but with our modifications, this overestimation is compensated and the modified BMW model gives free energy values of ca. 70 kJ/mol (Fig. 6A), in agreement with atomistic and MARTINI models. Our modified BMW model gives more accurate values and maintains the shape of the energy profile, improving the ability of the model to reproduce lipid flip-flop free energies.

Free energy of transferring a DPPC molecule from the bilayer into bulk water is of 75 kJ/mol for our modified BMW FF (Fig. 6B), and is in agreement with values obtained with atomistic models [41]. As observed for flip-flop, the free energy barriers for BMW-MARTINI DPPC desorption were significantly overestimated, giving a maximum of approx. 125 kJ/mol (Fig. 6B). Therefore, our modified FF represents an improvement since it better reproduces the free energy of flip-flop and desorption of lipids.

## 4. Conclusion

We assessed BMW-MARTINI in order to determine which structural and thermodynamical properties can be accurately described with this CG model. We found that for lipid monolayers compression isotherms showed the serious artifact of regions with negative surface pressure. In lipid bilayers, Mma and melting temperature values of PC lipids

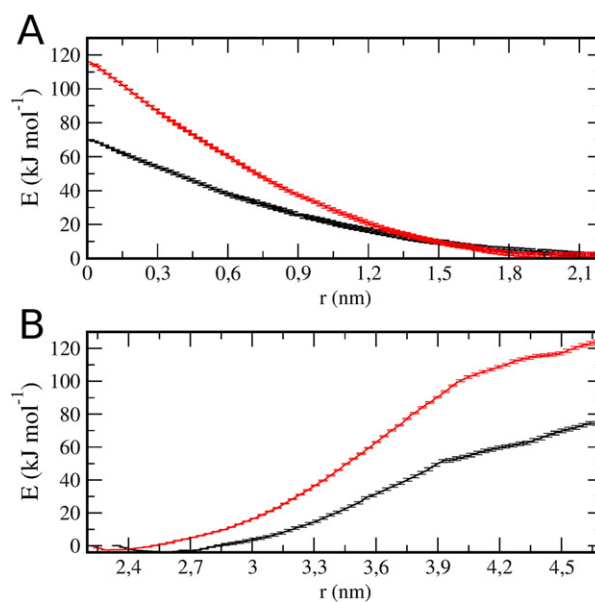


**Fig. 6.** PMFs for (A) flip-flop and (B) lipid desorption from the bilayer to bulk water of a DPPC molecule. The x-axis refers to the distance between the PO4 bead position and the bilayer center. Black line, our modified FF; red line, BMW-MARTINI. Error bars represent the standard error obtained with bootstrap analysis with g\_wham.

were not accurate either. Finally, molecular geometries of lipid molecules diverge from the expected based on all atoms simulations. We improve the performance for the items mentioned above by modifying beads interactions with water and by adjusting lipids geometries.

We were able to modify BMW-MARTINI FF to obtain a model that possesses proper treatment of electrostatics and is capable of reproducing the several important properties of the phospholipids systems. This should be a tool that allows lipidic system analysis at larger time and size scales.

## Transparency document

The [Transparency document](#) associated with this article can be found, in online version.

## Acknowledgements

This work was supported in part by the Consejo Nacional de Investigaciones Científicas y Tecnológicas (CONICET) (Grants 11220100100441 and 11220130100650CGI), the Agencia Nacional de Promoción Científica y Tecnológica (FONCYT, Argentina) (Grant PICT2012-2652), the Agencia Córdoba Ciencia and the Secretaría de Ciencia y Técnica (SECYT) of the Universidad Nacional de Córdoba (Grants 30720130100946CB, 0720150100684CB and 0920150100514CB). INFIQC and IIByT are jointly sponsored by CONICET and the universities Universidad Nacional de Córdoba. All calculations were performed with computational resources from CCAD - Universidad Nacional de Córdoba (<http://ccad.unc.edu.ar/>). MAV, MAP and VM are CONICET Career Members.

## Appendix A. Supplementary data

Supplementary data to this article can be found online at <http://dx.doi.org/10.1016/j.bbamem.2016.08.016>.

## References

- [1] Z. Wu, Q. Cui, A. Yethiraj, A new coarse-grained model for water: the importance of electrostatic interactions, *J. Phys. Chem. B* 114 (2010) 10524–10529.
- [2] S.J. Marrink, D.P. Tieleman, Perspective on the Martini model, *Chem. Soc. Rev.* 42 (2013) 6801–6822.
- [3] L. Darré, M.a.R. Machado, P.D. Dans, F.E. Herrera, S. Pantano, Another coarse grain model for aqueous solvation: WAT FOUR? *Journal of Chemical Theory and Computation* 6 (2010) 3793–3807.
- [4] S.J. Marrink, H.J. Risselada, S. Yefimov, D.P. Tieleman, A.H. de Vries, The MARTINI force field: coarse grained model for biomolecular simulations, *J. Phys. Chem. B* 111 (2007) 7812–7824.
- [5] W. Shinoda, R. DeVane, M.L. Klein, Zwitterionic lipid assemblies: molecular dynamics studies of monolayers, bilayers, and vesicles using a new coarse grain force field, *J. Phys. Chem. B* 114 (2010) 6836–6849.
- [6] S.O. Yesylevskyy, L.V. Schafer, D. Sengupta, S.J. Marrink, Polarizable water model for the coarse-grained MARTINI force field, *PLoS Comput. Biol.* 6 (2010), e1000810.
- [7] Z. Wu, Q. Cui, A. Yethiraj, A new coarse-grained force field for membrane-peptide simulations, *J. Chem. Theory Comput.* 7 (2011) 3793–3802.
- [8] S. Baoukina, D.P. Tieleman, Simulations of lipid monolayers, *Methods Mol. Biol.* 924 (2013) 431–444.
- [9] S. Baoukina, D.P. Tieleman, Computer simulations of lung surfactant, *Biochimica et Biophysica Acta* 1858 (10) (2016) 2431–2440.
- [10] L. Cwiklik, Tear film lipid layer: a molecular level view, *Biochimica et Biophysica Acta* 1858 (10) (2016) 2421–2430.
- [11] S. Baoukina, S.J. Marrink, D.P. Tieleman, Structure and dynamics of lipid monolayers: theory and applications, in: H. Press (Ed.), *Biomembrane Frontiers* 2009, pp. 75–99.
- [12] X. Periolo, S.J. Marrink, The Martini coarse-grained force field, *Methods Mol. Biol.* 924 (2013) 533–565.
- [13] J.P. Jambeck, A.P. Lyubartsev, Derivation and systematic validation of a refined all-atom force field for phosphatidylcholine lipids, *J. Phys. Chem. B* 116 (2012) 3164–3179.
- [14] S.W. Chiu, S.A. Pandit, H.L. Scott, E. Jakobsson, An improved united atom force field for simulation of mixed lipid bilayers, *J. Phys. Chem. B* 113 (2009) 2748–2763.
- [15] S.A. Pandit, S.W. Chiu, E. Jakobsson, A. Grama, H.L. Scott, Cholesterol surrogates: a comparison of cholesterol and 16:0 ceramide in POPC bilayers, *Biophys. J.* 92 (2007) 920–927.
- [16] S.A. Pandit, S.W. Chiu, E. Jakobsson, A. Grama, H.L. Scott, Cholesterol packing around lipids with saturated and unsaturated chains: a simulation study, *Langmuir* 24 (2008) 6858–6865.
- [17] J. Domanski, P.J. Stansfeld, M.S. Sansom, O. Beckstein, Lipidbook: a public repository for force-field parameters used in membrane simulations, *The Journal of membrane biology* 236 (2010) 255–258.
- [18] L. Martinez, R. Andrade, E.G. Birgin, J.M. Martinez, PACKMOL: a package for building initial configurations for molecular dynamics simulations, *J. Comput. Chem.* 30 (2009) 2157–2164.
- [19] S.L. Duncan, R.G. Larson, Comparing experimental and simulated pressure-area isotherms for DPPC, *Biophys. J.* 94 (2008) 2965–2986.
- [20] G. Bussi, D. Donadio, M. Parrinello, Canonical sampling through velocity rescaling, *J. Chem. Phys.* 126 (2007) 014101.
- [21] T. Darden, D. York, L. Pedersen, Particle mesh Ewald: an  $N \cdot \log(N)$  method for Ewald sums in large systems, *J. Chem. Phys.* 98 (1993) 10089.
- [22] S. Baoukina, L. Monticelli, S.J. Marrink, D.P. Tieleman, Pressure-area isotherm of a lipid monolayer from molecular dynamics simulations, *Langmuir* 23 (2007) 12617–12623.
- [23] V.M. Kaganer, E.B. Loginov, Crystallization phase transitions and phase diagram of Langmuir monolayers, *Phys. Rev. Lett.* 71 (1993) 2599–2602.
- [24] J.S. Hub, B.L. de Groot, D. van der Spoel, g\_wham—a free weighted histogram analysis implementation including robust error and autocorrelation estimates, *J. Chem. Theory Comput.* 6 (2010) 3713–3720.
- [25] S. Pronk, S. Pall, R. Schulz, P. Larsson, P. Bjelkmar, R. Apostolov, M.R. Shirts, J.C. Smith, P.M. Kasson, D. van der Spoel, B. Hess, E. Lindahl, GROMACS 4.5: a high-throughput and highly parallel open source molecular simulation toolkit, *Bioinformatics* 29 (2013) 845–854.
- [26] R. Baron, A.H. de Vries, P.H. Hunenberger, W.F. van Gunsteren, Comparison of atomic-level and coarse-grained models for liquid hydrocarbons from molecular dynamics configurational entropy estimates, *J. Phys. Chem. B* 110 (2006) 8464–8473.
- [27] D.M. Mitrinovic, A.M. Tikhonov, M. Li, Z. Huang, M.L. Schlossman, Noncapillary-wave structure at the water-alkane interface, *Phys. Rev. Lett.* 85 (2000) 582–585.
- [28] S. Diaz, F. Lairion, J. Arroyo, A.C. Biondi de Lopez, E.A. Disalvo, Contribution of phosphate groups to the dipole potential of dimyristoylphosphatidylcholine membranes, *Langmuir* 17 (2001) 852–855.
- [29] A. Iglic, *Advances in Planar Lipid Bilayers and Liposomes*, 2012.
- [30] S.J. Marrink, J. Risselada, A.E. Mark, Simulation of gel phase formation and melting in lipid bilayers using a coarse grained model, *Chem. Phys. Lipids* 135 (2005) 223–244.
- [31] J.F. Nagle, S. Tristram-Nagle, Lipid bilayer structure, *Curr. Opin. Struct. Biol.* 10 (2000) 474–480.
- [32] T. Chen, J.P. Acker, A. Eroglu, S. Cheley, H. Bayley, A. Fowler, M. Toner, Beneficial effect of intracellular trehalose on the membrane integrity of dried mammalian cells, *Cryobiology* 43 (2001) 168–181.
- [33] R. Koynova, M. Caffrey, Phases and phase transitions of the phosphatidylcholines, *Biochim. Biophys. Acta Rev. Biomembr.* 1376 (1998) 91–145.
- [34] N. Kucerka, M.P. Nieh, J. Katsaras, Fluid phase lipid areas and bilayer thicknesses of commonly used phosphatidylcholines as a function of temperature, *Biochim. Biophys. Acta* 1808 (2011) 2761–2771.
- [35] H.I. Petrache, S.W. Dodd, M.F. Brown, Area per lipid and acyl length distributions in fluid phosphatidylcholines determined by  $(2)H$  NMR spectroscopy, *Biophys. J.* 79 (2000) 3172–3192.
- [36] A. Raudino, F. Zuccarello, C. La Rosa, G. Buemi, Thermal expansion and compressibility coefficients of phospholipid vesicles: experimental determination and theoretical modeling, *J. Phys. Chem.* 94 (1990) 7.
- [37] A.-L. Kuo, C.G. Wade, Lipid lateral diffusion by pulsed nuclear magnetic resonance, *Biochemistry* 18 (1979) 2300–2308.
- [38] J.R. Sheats, H.M. McConnell, A photochemical technique for measuring lateral diffusion of spin-labeled phospholipids in membranes, *Proc. Natl. Acad. Sci. U. S. A.* 75 (1978) 4661–4663.
- [39] D. Mohammad-Aghaie, E. Mace, C.A. Sennoga, J.M. Seddon, F. Bresme, Molecular dynamics simulations of liquid condensed to liquid expanded transitions in DPPC monolayers, *J. Phys. Chem. B* 114 (2010) 1325–1335.
- [40] W.F. Bennett, D.P. Tieleman, Water defect and pore formation in atomistic and coarse-grained lipid membranes: pushing the limits of coarse graining, *J. Chem. Theory Comput.* 7 (2011) 2981–2988.
- [41] D.P. Tieleman, S.J. Marrink, Lipids out of equilibrium: energetics of desorption and pore mediated flip-flop, *J. Am. Chem. Soc.* 128 (2006) 12462–12467.